PHILOSOPHICAL TRANSACTIONS OF THE ROYAL SOCIETY A MATHEMATICAL, PHYSICAL & ENGINEERING SCIENCES

Ground-Based Observations Coordinated with Viking Satellite Measurements [and Discussion]

H. J. Opgenoorth, Sheila Kirkwood, A. S. Rodger and P. Rothwell

Phil. Trans. R. Soc. Lond. A 1989 **328**, 221-233
doi: 10.1098/rsta.1989.0033

Phil. Trans. R. Soc. Lond. A **328**, 221–233 (1989)
Printed in Great Britain

Ground-based observations coordinated with *Viking* satellite measurements

By H. J. Opgenoorth[1] and Sheila Kirkwood[2]

[1] *Swedish Institute of Space Physics, Uppsala Division, S-755 91 Uppsala, Sweden*
[2] *Swedish Institute of Space Physics, Box 812, S-98128 Kiruna, Sweden*

[Plates 1 and 2]

The instrumentation and the orbit of the *Viking* satellite made this first Swedish satellite mission ideally suited for coordinated observations with the dense network of ground-based stations in northern Scandinavia. Several arrays of complementing instruments such as magnetometers, all-sky cameras, riometers and doppler radars monitored on a routine basis the ionosphere under the magnetospheric region passed by *Viking*. For a large number of orbits the *Viking* passages close to Scandinavia were covered by the operation of specially designed programmes at the European incoherent-scatter facility (EISCAT). First results of coordinated observations on the ground and aboard *Viking* have shed new light on the most spectacular feature of substorm expansion, the westward-travelling surge. The end of a substorm and the associated decay of a westward-travelling surge have been analysed. EISCAT measurements of high spatial and temporal resolution indicate that the conductivities and electric fields associated with westward-travelling surges are not represented correctly by the existing models.

Introduction

As described by Hultqvist (1987, and this Symposium) the orbit and instrumentation of the *Viking* satellite were specially designed to study the physical processes occurring on high-latitude magnetic field-lines. Since the discoveries of the earlier *S*3-3 satellite at altitudes of several thousand kilometres, this region has been recognized as being at least as important as the far magnetotail for the acceleration of particles and production of forms and structures in the aurora.

The high-latitude regions of the ionosphere and magnetosphere are more or less permanently interconnected by a complex system of upward and downward directed currents flowing along the magnetic field-lines, carried mainly by cold electrons but, particularly during magnetospheric disturbances, containing a substantial proportion of energetic electrons and ions. If, during magnetospheric disturbances, the field-aligned current density exceeds a certain instability threshold, a number of processes are initiated. Plasma waves are generated, which are directly measurable as so-called auroral kilometric radiation (AKR) and as a wide band of emissions at other frequencies in both electrostatic and electromagnetic modes. Such plasma waves can accelerate or decelerate magnetospheric electrons and ions either directly, by wave–particle interaction, or lead to secondary build-up of large-scale, easily measurable potential structures, several hundred kilometres in size and, typically, with a potential difference of *ca.* 10 keV.

The resulting precipitation of particles into the polar ionosphere below creates, depending on its energy and spatial structure, inhomogeneous ionospheric conductivities. Magnetospheric electric fields and currents can drive ionospheric currents, which build up secondary polarization electric fields and field-aligned currents, finally resulting in very complicated three-dimensional current configurations, different for each type of auroral precipitation.

From the above description it is obvious that, even if individual data from satellites and ground-based instruments deliver the basis for a large number of interesting studies, a complete picture of this complicated coupling process can only be revealed by a combination of continuous ground-based measurements within extended areas (magnetometers, riometers, Doppler radars, auroral cameras, etc.) and detailed, high-resolution measurements of plasma parameters, *in situ* in the magnetosphere by satellites (e.g. *Viking*) and remotely probed in the ionosphere by incoherent-scatter radars (e.g. European incoherent scatter (EISCAT)).

During the *Viking* mission in 1986 a large number of ground-based instruments monitored the high-latitude ionosphere over northern Scandinavia. A cross-shaped array of magnetometers (Lühr *et al.* 1984) and two systems of bistatic coherent Doppler radars (Nielsen 1982; Nielsen *et al.* 1983) recorded the two-dimensional ionospheric currents and plasma convection, respectively. Networks of riometers, all-sky cameras and photometers detected energetic particle precipitation and optical auroral emissions. EISCAT, the tristatic European incoherent-scatter radar facility probed ionospheric plasma parameters such as electron density, electron and ion temperatures, the vector electric field and, at times, even neutral wind profiles for most of the *Viking* passages close to Scandinavia. A combined effort by all six EISCAT associate countries allowed about 25% of EISCAT's annual special programme time to be dedicated to observations coordinated with *Viking*. Three experiment modes for different geophysical conditions were designed and put into operation by an international working group. The programme modes contained a stationary antenna pointing direction along the Tromsö field-line for local, high-time-resolution measurements of plasma parameters during active aurora, a small scan between Kiruna and Tromsö for a medium-time-resolution, medium-range-coverage of moderately dynamic structures and a 16 point horizon-to-horizon scan for studies of global processes (for details of the EISCAT–*Viking* coordination see Opgenoorth *et al.* 1989).

An interesting problem for coordinated magnetospheric and ionospheric observations is that the original particle precipitation and current flow, which first excites and is then modified by the processes at an altitude of several hundred kilometres, is not homogeneous, but, particularly during magnetospheric substorm activity, highly dynamic and spatially inhomogeneous. One model of the three-dimensional current flow during a magnetospheric substorm, which is still generally accepted, is illustrated by the sketch in figure 1 (from McPherron *et al.* 1973). This so-called substorm current-wedge is thought to be superimposed on the quiet-time system of field-aligned currents, consisting of extended pairs of sheet currents of opposite directions in the evening and morning sector of the auroral oval.

If the current across the magnetospheric tail is driven unstable by an increased energy input from the solar wind plasma, it shortcircuits along the magnetic field-lines into the polar ionosphere, where an increased ionospheric current, the westward substorm electrojet, is easily detectable by ground-based magnetometers. The substorm leads to drastically increased particle precipitation in the affected part of the auroral oval. Particularly at the western edge of the current wedge, where precipitating electrons carry upwardly directed field-aligned

PHILOSOPHICAL TRANSACTIONS OF THE ROYAL SOCIETY A MATHEMATICAL, PHYSICAL & ENGINEERING SCIENCES

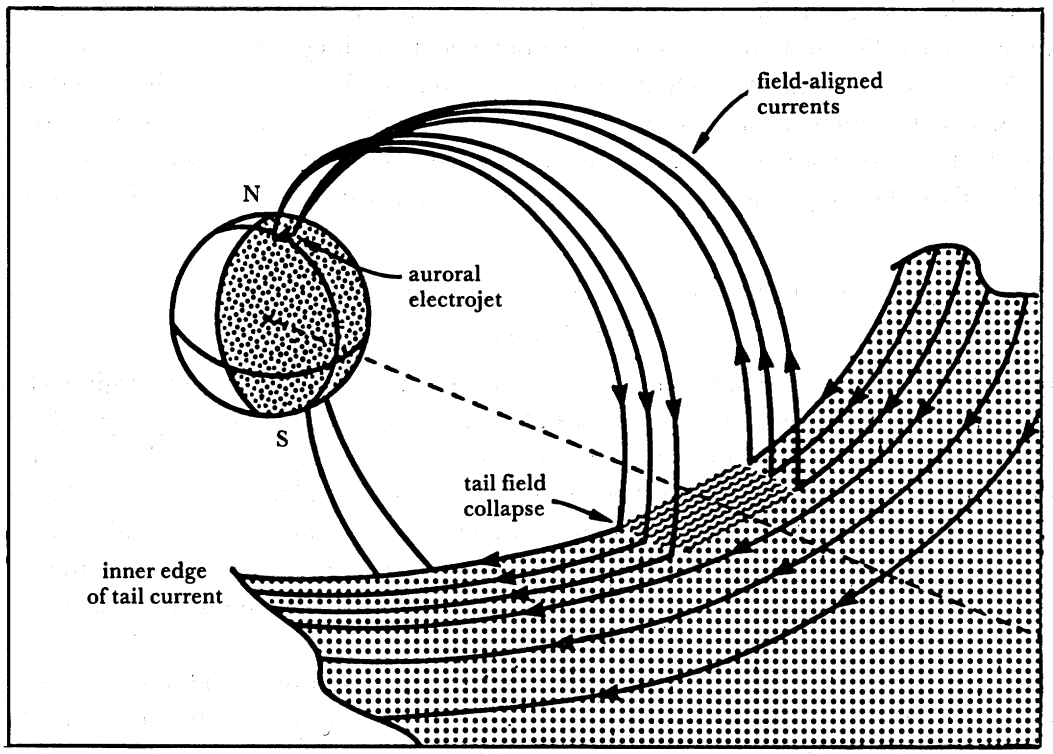

FIGURE 1. Sketch of the magnetospheric current flow during the onset of a magnetospheric substorm (from McPherron *et al.* 1973).

current, dramatic auroral features develop. The magnetic vorticity produced by the strong localized current wraps the magnetic field-lines in such a way that the footprints of the particle precipitation along those lines (visible as aurora) resemble a large spiral. In the later course of the substorm the current wedge expands to the flanks of the magnetosphere, resulting in a westward motion of the auroral spiral. This so-called westward-travelling surge (WTS) is probably the most dramatic feature of the magnetospheric substorm. Equivalent processes under the eastern portion of the substorm current wedge are much more diffuse, mainly because of the different nature of the current carrying particles there.

The gross ionospheric and field-aligned current flow inside the WTS and its association with the substorm current wedge was deduced some years ago from analysis of global magnetometer network data (see, for example, Kamide & Akasofu 1975). More detailed analysis using data from denser magnetometer chains (Kisabeth & Rostoker 1973) and networks (Baumjohann *et al.* 1981; Inhester *et al.* 1981; Opgenoorth *et al.* 1983) improved the understanding of the ionospheric part of the current flow and clarified the relative roles of the horizontal ionospheric Hall and Pedersen conductivities (see Opgenoorth *et al.* 1983). However, the above models are unsatisfactory to the extent that both the overall ionospheric conductivity distribution and the electric field inside the auroral structures had to be assumed and were then fitted to the observed magnetic disturbances on the ground. The existing models can certainly be improved with better measurements of the conductivity and electric field distribution, which are now available from satellites and the ground-based incoherent-scatter facilities.

In the following we shall report two studies dealing with aspects of WTSs. The first study

(Opgenoorth *et al.* 1989) describes the observations of a WTS close to the end of a substorm expansion. According to Baumjohann (1986) our understanding of the onset of the substorm expansion phase is relatively well developed, but our understanding of how and why a substorm decays, often before all available magnetospheric energy is released, is still very limited. In the second study we will present results of high resolution EISCAT measurements of electric fields and conductances in association with WTSs and break-up aurora (Kirkwood *et al.* 1989).

The decay of a westward-travelling surge

Observations

On 9 April 1986, the *Viking* satellite passed the high-latitude auroral region close to Scandinavia between about 18h05 and 18h25 U.T. (orbit 258). The sequence of imager pictures in figure 2, plate 1, shows that during this evening sector passage *Viking* encountered a bright surge-like auroral feature, located several hundred kilometres off the Norwegian coast. The shape of the auroral form resembles a WTS, however, no westward motion (typically 1 km s^{-1} for a WTS) can be identified. During the time interval of six minutes, when the auroral form is in the field-of-view of the *Viking* imager (only the first three minutes are shown here), a WTS should have progressed by at least 300–400 km.

Just after the ultraviolet (UV) imager lost sight of the auroral oval, the satellite passed the magnetic field-lines which map to the wake of the auroral form (see figure 2). It should, however, be noted that the bright auroral features, which can be seen inside the spiral at 18h08 U.T., have almost completely decayed by the time of the satellite pass through the same field-lines at 18h18 U.T. (compare (*a*) and (*d*) frame of figure 2). The stacked diagram in figure 3 shows the *Viking* measurements of electron precipitation in two representative energy channels (0.2 and 3.87 keV) and the north–south component of the electric field.

The *Viking* observations in figure 3 contain features typical of the evening sector of the auroral oval. Southward of the auroral oval, from 64° to 66° invariant latitude, the particle precipitation is soft, indicating diffuse subvisual aurora, and the electric field is northward directed. At about 66° latitude the precipitation becomes harder. The magnetic field observations (data not shown here) indicate a sheet of downward field-aligned current, north of which the northward directed electric field also reaches its highest values.

The satellite then enters the wake of the auroral form, where the observations clearly differ from the typical undisturbed evening sector pattern. The northward electric field is depressed, and the particle precipitation is clearly harder than in the diffuse aurora. However, the electron energy spectra in this region show no clear peak which could indicate field-aligned acceleration by potential drops above the *Viking* orbit. The electric field data shows no indication of a potential drop below the satellite either. This type of spectral shape, stemming solely from central plasma sheet particle acceleration was recognized by Meng *et al.* (1978) as typical for the central WTS regions. Apparently, since *Viking* passes to the east of the main spiral, we do not observe a pronounced tail of very energetic particles in the spectra. The magnetic data indicates a disturbed upward field-aligned current flow out of the wake of the auroral form, which should be expected if the spiral formed the westward edge of a substorm current wedge.

Even further north, at about 71° (from 18h19 to 18h20 U.T.), *Viking* appears to pass through a W-shaped potential structure, appearing in the electric field data as alternating

PHILOSOPHICAL TRANSACTIONS OF THE ROYAL SOCIETY A MATHEMATICAL, PHYSICAL & ENGINEERING SCIENCES

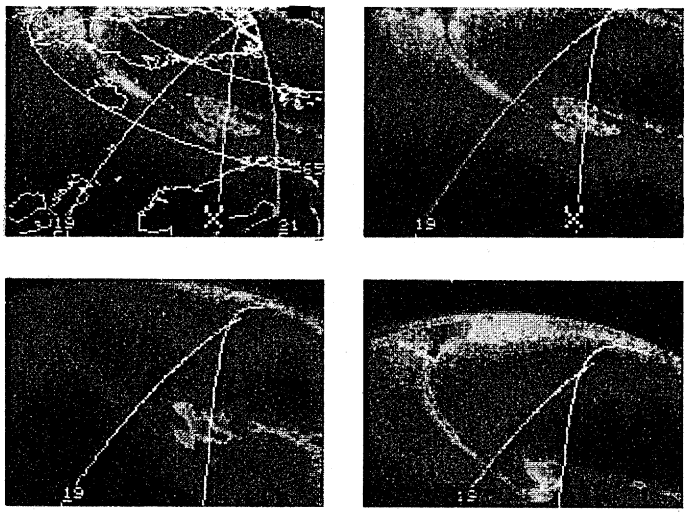

FIGURE 2. Sequence of *Viking* UV-images during orbit 258 on 9 April 1986. In the first two frames the magnetically projected footprint of the *Viking* orbit (position marked with X) is indicated together with the 19h00 and 21h00 magnetic local time (MLT) meridians and map outline. Top left and top right frames are at 18h08:25 U.T.; bottom left is at 18h09:05 U.T.; bottom right is at 18h11:05 U.T.

(*Facing p.* 224)

PHILOSOPHICAL TRANSACTIONS OF THE ROYAL SOCIETY A MATHEMATICAL, PHYSICAL & ENGINEERING SCIENCES

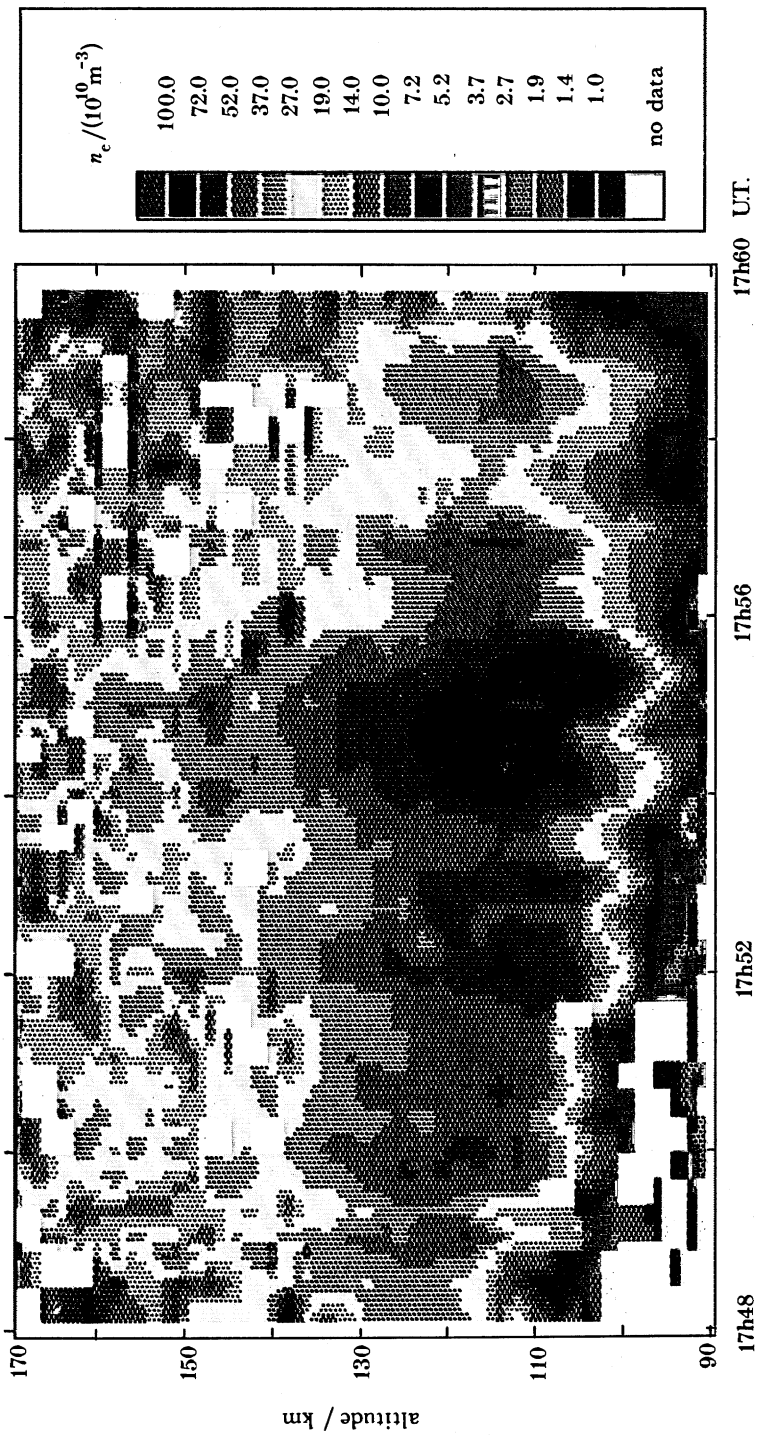

FIGURE 6. Colour-coded plot of ionospheric electron density against altitude and time observed with the E-layer multipulse part of the EISCAT programme UHF1 during the substorm of 9 April 1986.

PHILOSOPHICAL TRANSACTIONS OF THE ROYAL SOCIETY A MATHEMATICAL, PHYSICAL & ENGINEERING SCIENCES

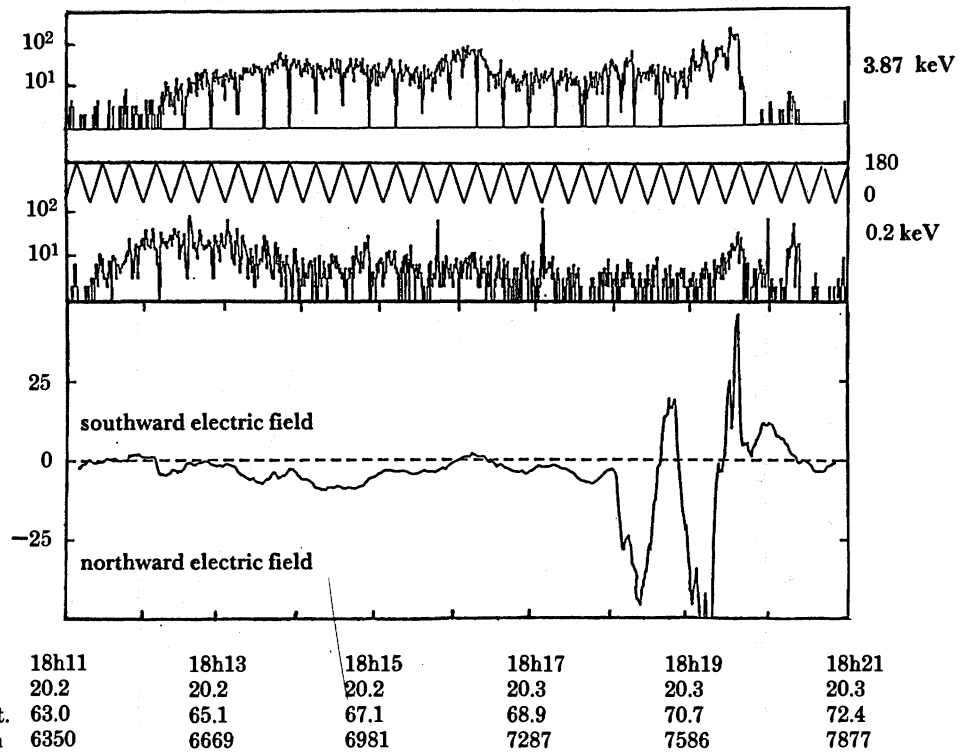

FIGURE 3. *Viking* observations of electron precipitation in two representative energy channels (0.2 and 3.87 kV) and the north–south component of the electric field during orbit 258 on 9 April 1986. Below the time axis in U.T. we give also MLT, invariant latitude and satellite altitude.

sharp northward and southward excursions. The integrated potential drop within this structure (the equipotential contours are expected to close below) is slightly over 5 kV, which is in good agreement with simultaneous *Viking* observations of upwardly directed 5 keV ion beams. The increased 3.87 keV electron flux after 19h19 U.T. indicates that the potential structure continues even above the satellite, at least for the second V of the W-shaped structure. An example of the complete electron energy spectra in this region is given in figure 4. The peak in the flux of precipitating electrons (10° pitch angle) at 5.6 keV indicates field-aligned acceleration above the satellite. It can be concluded that *Viking* must have passed exactly through the middle of a potential drop of totally 11 kV, associated with the bright arc at the northern edge of the spiral's wake. The satellite's magnetic field measurements at this latitude indicate a strong sheet of upwardly directed current flow.

The *Viking* observations can be summarized as typical evening sector auroral zone features (northward electric field, soft diffuse precipitation associated with a downward field-aligned current sheet to the south and a discrete auroral arc, associated with a V-shaped potential drop and a sheet of upward current to the north) with a superimposed disturbance pattern typical of a WTS (suppression of the vector electric field, more energetic particle precipitation without a clear peak in the energy spectrum and a distributed upward field-aligned current flow). However, we still have the puzzling observation that the surge does not travel.

The magnetograms from the EISCAT magnetometer cross in figure 5*a* show that the *Viking* observations are connected to a substorm (negative x-component deflection), occurring in the decline of a large pre-existing positive bay caused by a global eastward electrojet. The substorm

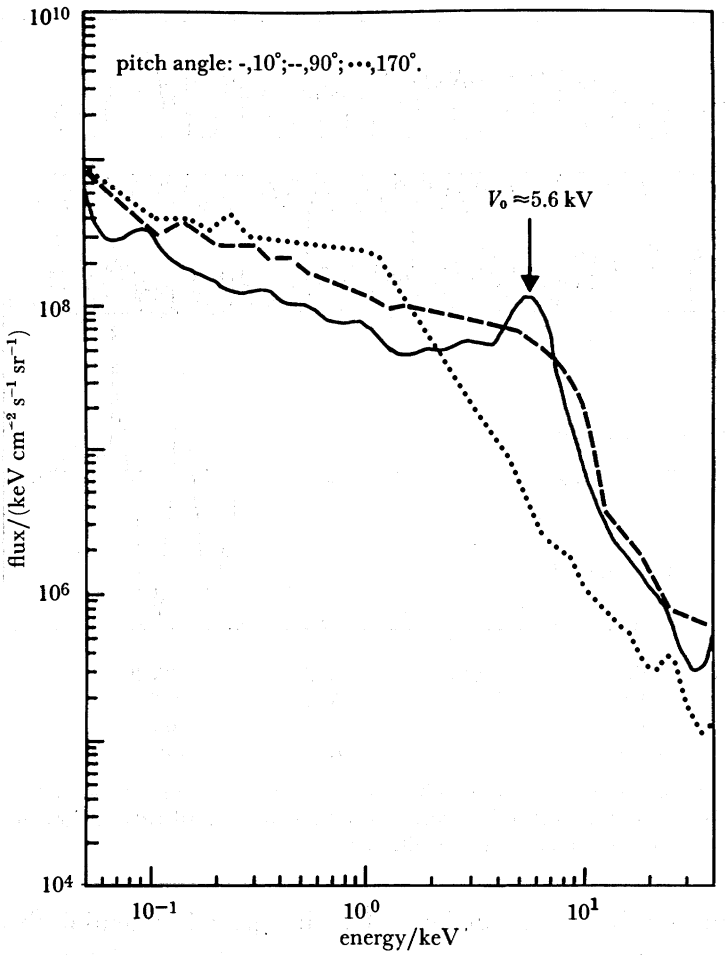

FIGURE 4. Electron energy spectra for different pitch angles observed by the *Viking* V3 experiment during the time interval 18h19–18h20 U.T. on 9 April 1986 (orbit 258).

onset took place at about 17h54 U.T. and by the time of the *Viking* passage the main magnetospheric energy release has certainly ceased. High-resolution plots of the magnetic *x*- and *y*-components in figure 5*b*, *c* reveal that the disturbance pattern at substorm onset (marked by the vertical broken line) resembles the typical magnetic signatures of a WTS (Tighe & Rostoker 1981; Opgenoorth *et al.* 1983). A negative *x*-onset at the northernmost stations and a positive *x*-onset at the stations to the south are associated with a positive deviation of the *y*-component at all stations. The positive *y*-onset is delayed by almost 2 min from Kevo to Kilpisjärvi, an east–west distance of about 250 km, indicating a westward propagation at 2 km s^{-1}. A similar propagation of a region of eastward directed plasma drifts (indicating westward current flow) can be seen from 17h54 to 17h58 U.T. in the two-dimensional data-set of the STARE radar (data not shown here, see Opgenoorth *et al.* (1989) for details; STARE is the Scandanavian twin-auroral radar experiment). Evidence that the westward substorm expansion continues is provided by the magnetometer on Jan Mayen (located under the stationary auroral spiral in the *Viking* UV-images in figure 2), which records the sudden onset of a negative *x*-disturbance at 18h10 U.T., lasting for only 5 min. The disturbance of the westward substorm electrojet declines then simultaneously along the affected portion of the oval.

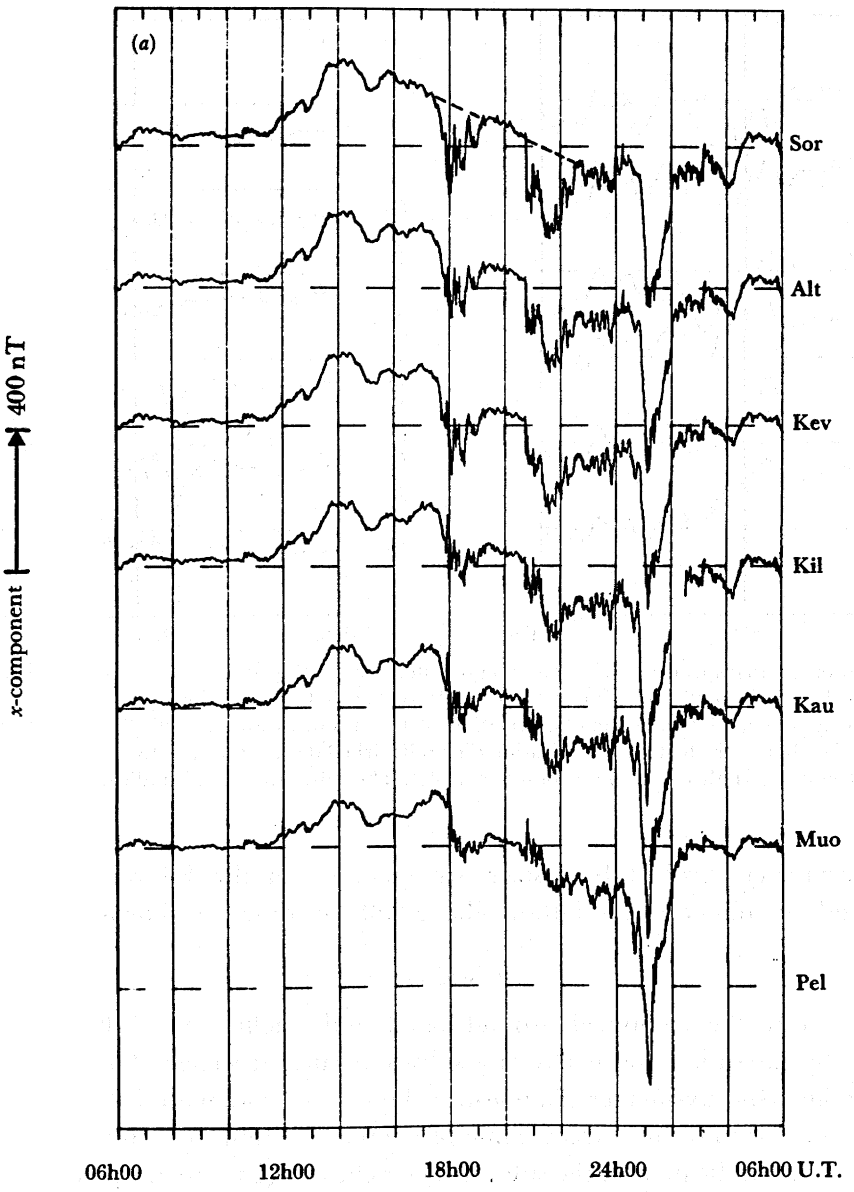

FIGURE 5(*a*). For description see page 228.

The EISCAT radar operated during this night in the field-aligned high-time-resolution mode UHF1 (ultra-high frequency). From the altitude distribution of ionospheric electron density in figure 6, plate 2, it can be seen that the first auroral activity started at 17h50 U.T., when both STARE and the magnetometers recorded the first disturbance of the eastward electrojet. The expanding westward edge of the substorm current wedge hits the radar beam between 17h54:30 and 17h55:00 U.T., which is in agreement with EISCAT's position with respect to the magnetometer stations discussed above. The dramatic increase of electron density during this maximum disturbance period affects both the highest and lowest E-layer altitudes, which indicates a general increase of precipitating particle fluxes of all energies, as is typically observed within a WTS (Meng *et al.* 1978). Other features associated with the WTS in the

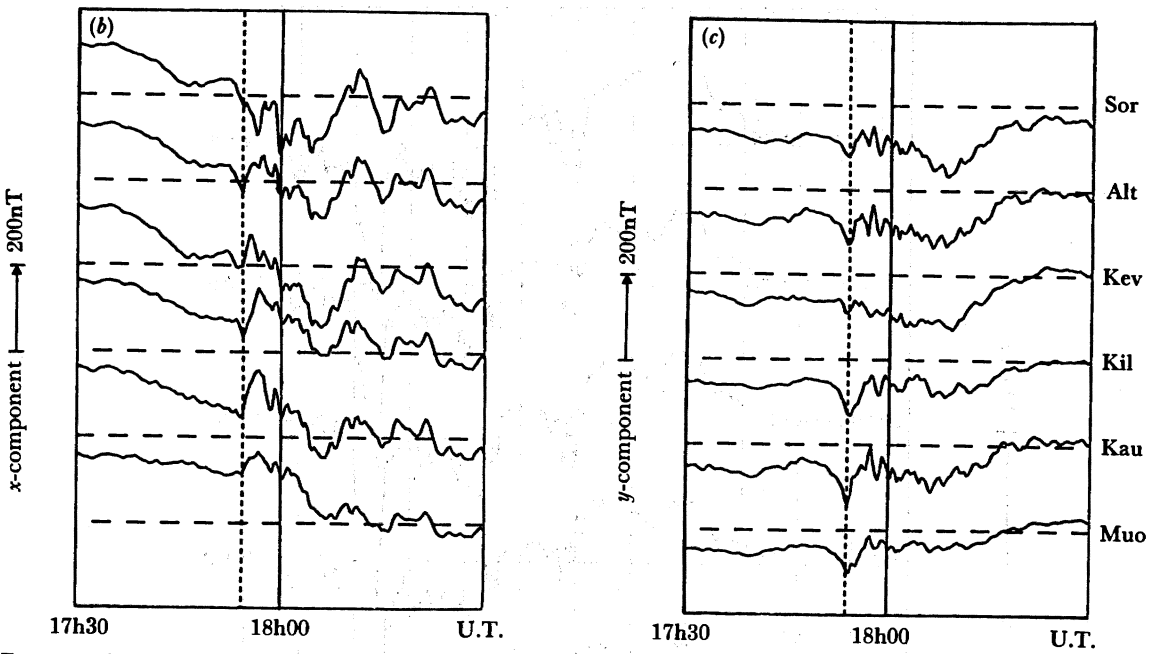

FIGURE 5. Stacked magnetograms from the EISCAT magnetometer cross (Sor is Sorøya, Alt is Alta, Kev is Kevo, Kil is Kilpisjärvi, Kau is Kautokeino, Muo is Muonio, Pello (Pel) left out) for the substorm on 9 April 1986. (*a*) Overview *x*-component plot indicating the relation of the substorm around 18h00 U.T. to preceding bay activity, a broken line in the first panel indicating the undisturbed decay of the positive bay. (*b*) High-resolution *x*-component plot. (*c*) High-resolution *y*-component plot. The substorm onset is indicated by a broken line in (*b*) and (*c*).

ionospheric parameters probed by EISCAT are increases in the F-layer electron and ion temperature and an enhanced ion outflow above 250 km (data not shown here).

Discussion

In this case study the combined ground-based and satellite data allowed a complete observation of the expansion and decay of a substorm current wedge. The initially puzzling observation by the *Viking* UV-imager of a non-travelling WTS could, with the help of the ground-based network, be put into the correct frame of reference within the substorm development. Both data-sets clearly indicate that the substorm current wedge is superimposed on the typical local sector three-dimensional current flow determined by the direction of the region I and region II field-aligned current sheets. The current wedge apparently expands until the magnetospheric energy release is terminated, and then the substorm disturbance decays simultaneously along the whole affected portion of the auroral oval.

The WTS appears to remain stationary as long as westward current flow is maintained in the decaying substorm current wedge. Therefore the observation of standing surges in satellite images should be at least as common as the observation of WTSs, which is in fact the case in the *Viking* UV-imager data set (J. S. Murphree, personal communication). However, the standing surge seems to differ from the travelling one only by a general decrease in intensity and amplitude of the associated features. No qualitatively new physical process appear to be involved with the stationary substorm surge (SSS).

Ionospheric conductivities, electric fields and neutral winds associated with substorm auroras

As mentioned in the introduction, models of ionospheric current flow in association with substorm aurora have so far been based on relatively crude assumptions of conductivities and electric fields within the bright auroral forms. In regions of intense particle precipitation the increased ionospheric conductivity leads to an effective suppression of the electric field by polarization effects, usually to below the threshold needed for the excitation of ionospheric plasma waves, which are the main agents for the detection of plasma drifts with the coherent radar technique. During the International Magnetospheric Study (IMS) Baumjohann *et al.* 1981), Inhester *et al.* (1981) and Opgenoorth *et al.* (1983) used electric field data from the coherent STARE radar as input for their model calculations. Therefore they were, inside the bright auroral structures, free to assume any electric field of less than 15 mV m^{-1} in any arbitrary direction to match the observed magnetic disturbances on the ground. Their model conductivity distribution outside the auroral forms was fitted to the electric and magnetic field observations, but inside the aurora was based mainly on a small number of rocket measurements. Opgenoorth *et al.* (1983), for example, found that inside the substorm aurora an electric field of 10 mV m^{-1} and a Hall and Pedersen conductivity of 25 S and 20 S, respectively, reproduced the observed magnetic disturbance on the ground reasonably well.

As the incoherent-scatter technique allows the detection of even small electric fields and the derivation of the real ionospheric conductivity, it should be possible to improve the models of current flow in active aurora. With the help of *Viking* UV-images and the all-sky camera's data Kirkwood *et al.* (1988) selected seven substorm events close to the EISCAT radar. For simplicity we shall concentrate in this review on only six events.

From the primary EISCAT measurements of ionospheric electron density profiles, height-integrated ionospheric Hall and Pedersen conductivities were calculated according to standard equations (see, for example, Kato 1980) and using updated assumptions for the collision frequencies (Kirkwood *et al.* 1988). The temporal development of the height-integrated Hall conductivity Σ_H and the Hall to Pedersen conductivity ratio Σ_H/Σ_P for the six events are displayed in the lower panels of figure 7. As mentioned before, the field-aligned mode of the EISCAT experiment allows for an optional choice between continuous measurements of the undisturbed F-region $\boldsymbol{E}\times\boldsymbol{B}$ ion drift-velocity and alternating E-region and F-region drift measurements. In the E-region the ion drift is affected by both the electric field and the neutral wind drag so that the latter option will, under favourable conditions, result in the additional measurement of an altitude profile of neutral wind vectors (at the cost of uninterrupted electric field components and, when possible, also the horizontal ion drifts at 118 km altitude are given in the upper panels of figure 7.

Without going too much into details of the observations during the selected events one can immediately recognize that the IMS models for the current flow in substorm aurora have clearly underestimated the ionospheric conductivity and overestimated the electric field within the bright aurora itself. The observed height integrated Hall conductivities reach about 80 S in all cases, in the wake of the WTS on 1 December 1986 even well above 100 S. This is higher by a factor of 3–4 than assumed in the models discussed above. However, the EISCAT data also shows that the model assumptions on the electric field strength inside auroral structures were wrong by about the same factor in the opposite direction. The electric field observed by EISCAT

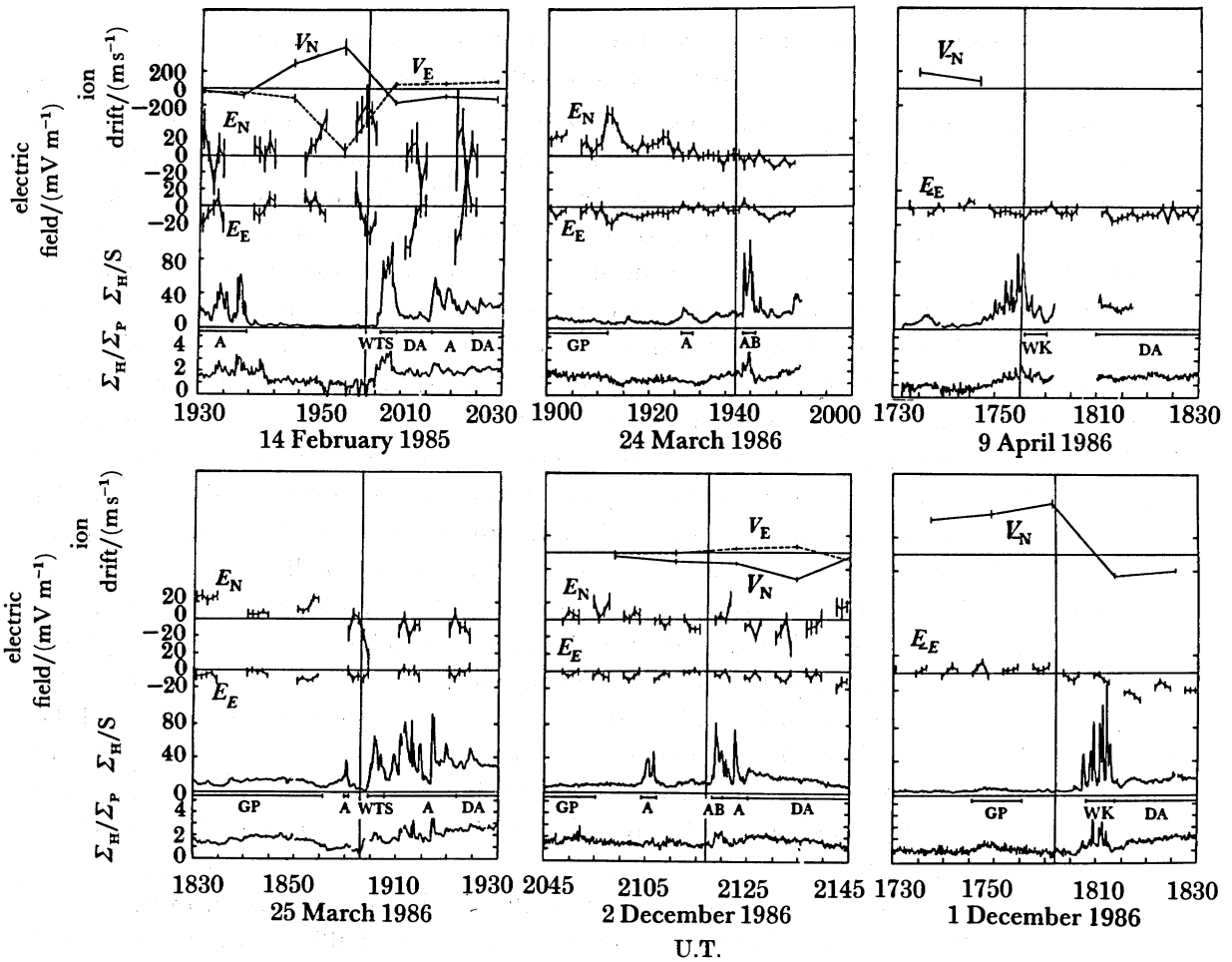

FIGURE 7. EISCAT measurements for six cases of substorm aurora. The parameters shown for each case are from the top: vector ion drift at 118 km altitude, vector electric field, Hall conductivity and ratio of Hall to Pedersen conductivity. Features partially referred to in the text are marked by GP (growth phase); A (discrete auroral arcs); DA (diffuse aurora); WTS (westward travelling surge); AB (auroral break-up) and WK (southern wake of the WTS).

is in all cases well below 5 mV m^{-1}, while the models assumed 10 mV m^{-1}, i.e. just below the STARE threshold of 15 mV m^{-1}. It can therefore be concluded that the models by Inhester *et al.* (1981), Baumjohann *et al.* (1981) and Opgenoorth *et al.* (1983) describe the gross three-dimensional current flow correctly within the spatial resolution of STARE and ground-based magnetometers.

Nevertheless, the EISCAT conductivity data in figure 7 still leave us with two major problems. The first problem is obvious and has up to now only been neglected because of insufficient spatial resolution of ground-based instruments; the EISCAT conductivity data is extremely variable, which indicates, as active aurora is very dynamic, that the horizontal conductivity distribution in active aurora, particularly in the southern wake of the WTS, is much more inhomogeneous than previously assumed. Field-aligned current flow is expected to develop at sharp gradients of the horizontal conductivity. Thus the real three-dimensional current flow inside a WTS must be considerably more complicated than assumed in the gross model calculations.

The second problem is less obvious and has not yet been considered in any WTS study so far. The extremely high ionospheric conductivities inside active aurora as measured by EISCAT allow even a small neutral wind to drive strong ionospheric currents effectively. In the models discussed above the neutral wind has been neglected, mainly because no measurements of its velocity and direction were available. The data presented in figure 7 clearly indicates the presence of strong neutral winds up to several 100 m s^{-1}, which must play an important part in the generation of ionospheric substorm current flow.

These new EISCAT measurements, which have to large extent been selected on the basis of *Viking* UV-images, show that even if we may have understood some basic features of the isolated magnetospheric substorm, which can be considered as relatively atypical, we are still only beginning to make complete measurements of the electrodynamics involved in normal substorms, i.e. those which occur in sequences or are imbedded in generally increased magnetospheric activity. It will be interesting to continue studies with the help of this type of data-set. The more data we collect the more we realize the complexity of the ionosphere's active coupling to the magnetosphere. Now we have to understand not only the magnetospheric reactions on secondary field-aligned currents driven by the ionospheric electric field through divergences in the horizontal currents, but also the reaction to neutral wind-generated current flow. While the former mechanism is probably 'known' by the magnetosphere, because most of the electric fields are of magnetospheric origin, the latter process must, in fact, actively disturb magnetospheric processes.

CONCLUSIONS

Out of the vast amount of coordinated data we have presented two studies, which demonstrate the possibilities of the combined data-sets from ground-based instrument arrays, including an incoherent-scatter facility and a magnetospheric satellite. Hopefully we have shown that the combination makes the data both quantitatively and qualitatively superior to previous data-sets from the same region. Apart from the cases described here scientists from the EISCAT–*Viking* coordination working group are studying different aspects of convection and precipitation boundaries seen by *Viking* and EISCAT, the effects of potential drops (measured by *Viking*) on particle precipitation at *Viking* and at ionospheric altitudes (calculating electron spectra above the ionosphere from EISCAT electron density profiles), a case of coordinated observations by *Viking*, the Aureld-Vip rocket and EISCAT along the same magnetic field-line (Sandahl *et al.* 1987), the development of transpolar arcs etc. The data-set of ground-based and *Viking* data, gathered during 1986, will easily keep us occupied for many more years.

The work presented here would not have been possible without the help of many energetic and far-sighted scientists in the *Viking* science team and the working group for EISCAT–*Viking* coordination, particularly G. Gustaffson and R. Pellinen, who in an early planning stage of the satellite project constantly pointed out the importance of coordinated ground-based observations and for the first time in space science history included the ground-based instrumentation as a principal experiment in the satellite mission. The staff at the *Viking* control centre and the EISCAT facility have contributed to the successful coordination between EISCAT and *Viking*. The EISCAT Scientific Association is supported by CNRS of France, SA of Finland, MPG of Germany, NAVF of Norway, NFR of Sweden and SERC of Great Britain. The *Viking*

PHILOSOPHICAL TRANSACTIONS OF THE ROYAL SOCIETY A MATHEMATICAL, PHYSICAL & ENGINEERING SCIENCES

project was managed and operated by the Swedish Space Corporation under contract from the Swedish Board for Space Activities and the construction and operation of the UV-imager were supported by the NRC and NSERC of Canada. The work of both authors is funded by the Swedish NFR.

References

Baumjohann, W. 1986 Some recent progress in substorm studies. *J. Geomagn. Geoelect., Kyoto* **38**, 633–651.

Baumjohann, W., Pellinen, R. J., Opgenoorth, H. J. & Nielsen, E. 1981 Joint two-dimensional observations of ground magnetic and ionospheric electric fields associated with auroral zone currents: current systems associated with local auroral break-ups. *Planet. Space Sci.* **29**, 431–447.

Hultqvist, B. 1987 The *Viking* project. *Geophys. Res. Lett.* **14**, 379–383.

Inhester, B., Baumjohann, W., Greenwald, R. A. & Nielsen, E. 1981 Joint two-dimensional observations of ground magnetic and ionospheric electric fields associated with auroral zone currents: 3. Auroral zone currents during the passage of a westward travelling surge. *J. Geophys.* **49**, 155–162.

Kamide, Y. & Akasofu, S.-I. 1975 The auroral electrojet and global auroral features. *J. geophys. Res.* **80**, 3585–3602.

Kato, S. 1980 Dynamics of the upper atmosphere. Dordrecht: Reidel.

Kirkwood, S., Opgenoorth, H. J., & Murphree, J. S. 1989 Ionospheric conductivities, electric fields and currents associated with auroral substorms measured by the EISCAT radar. (In the press.)

Kisabeth, J. L. & Rostoker, G. 1973 Current flow in auroral loops and surges inferred from ground-based magnetic observations. *J. geophys. Res.* **78**, 5573–5584.

Lühr, H., Thürey, S. & Klöcker, N. 1984 The EISCAT-mangetometer cross. *Geophys. Surv.* **6**, 305–315.

McPherron, R. L., Russell, C. T. & Aubry, M. P. 1973 Satellite studies of magnetospheric substorms on August 15, 1968: 9. Phenomenological model for substorms. *J. geophys. Res.* **78**, 3131–3149.

Meng, C.-I., Snyder, A. L. & Kroehl, H. W. 1978 Observations of auroral westward travelling surges and electron precipitation. *J. geophys. Res.* **83**, 575–585.

Nielsen, E. 1982 The STARE system and some of its applications. In *The IMS Source Book* (ed. C. T. Russell & D. J. S. Southwood), pp. 213–224. Washington: American Geophysical Union.

Nielsen, E., Güttler, W., Thomas, E. C., Stuart, C. P., Jones, T. B. & Hedberg, Å, 1983 A new radar auroral backscatter experiment. *Nature, Lond.* **304**, 712–714.

Opgenoorth, H. J., Pellinen, R. J., Baumjohann, W., Nielsen, E., Marklund, G. & Eliasson, L. 1983 Three-dimensional current flow and particle precipitation in a westward travelling surge (observed during the Barium-Geos rocket experiment). *J. geophys. Res.* **88**, 3138–3152.

Opgenoorth, H. J. *et al.* 1989 Coordinated observations with EISCAT and the *Viking* satellite – the decay of a westward travelling surge. (Submitted.)

Sandahl, I., Steen, Å., Pellinen-Wannberg, A., Holback, B., Soraas, F. & Murphree, J. S. 1987 First results from the *Viking* associated Aureld-VIP rocket and EISCAT campaign. In *Proc. 8th ESA symposium on European rocket and balloon programmes and related research*, Sunne, Sweden, 17–23 May 1987, **ESA SP-270**, 50–60.

Tighe, W. G. & Rostoker, G. 1981 Characteristics of westward travelling surges during magnetospheric substorms. *J. Geophys.* **50**, 51–67.

Discussion

A. S. Rodger (*British Antarctic Survey, Cambridge, U.K.*). It is generally accepted that, for a substorm to occur, a major reconfiguration of the magnetospheric tail must take place with the formation of a new neutral point possibly near 20 R_E†. Perhaps the key signature is the occurrence of a Pi2 geomagnetic pulsation at the beginning of the onset phase. It now appears that all auroral brightenings are being attributed to the substorm process. However, it is possible to enhance the level of light emission in the auroral oval, as would be detected by all-sky cameras or the *Viking* imager, by a variety of less catastrophic processes which are not associated with the major collapse of the magnetotail. Does Dr Opgenoorth consider that there is a need to define a substorm more precisely? Can he comment upon the different types of auroral brightening that do not appear to be associated with the 'classic' substorms?

† $R_E = 6.37 \times 10^6$ m.

H. J. Opgenoorth. I agree that the term 'substorm' confuses many scientists and is sometimes not clear even in the literature. Auroral disturbances seem to behave like substorms down to very small intensities and scale sizes (with substorm meaning the formation of an expanding current wedge, releasing magnetospheric energy in the ionosphere).

Akasofu tended to call such auroral intensifications 'pseudo-substorms', because they lacked the large-scale expansion features and Pi2 onset signatures at mid-latitude. However, better measurements have shown that small substorms display the same features as large ones, just more localized. Pi2 activity occurs often only locally or down to subauroral latitudes.

The latest attempt to unify different views on 'the substorm' is a paper by Rostoker *et al.* (1988) which, however, already now seems to have been overthrown by Rostoker himself and others based on new results of the *Viking* mission. I am afraid that it is too early for substorm physicists to settle down with a clear picture.

P. Rothwell (*University of Sussex, U.K.*). Some years ago, Risto Pellinen and I compared WTSS recorded with his all-sky cameras (5 pictures per minute) with our all-sky televisions (25 pictures per second). The TV records showed that the individual arcs in a surge moved eastward, but that new arcs brightened successively to the west of the existing arcs. This effect could explain why the *Viking* WTSS apparently remained stationary, given the right combination of arc eastward drift velocities and rate of appearance of new arcs at the westward edge of the surge.

H. J. Opgenoorth. I do fully agree that the motion of individual auroral structures within the WTS is not westward, but often eastward, as would be expected for an $\boldsymbol{E}\times\boldsymbol{B}$ drift in the southward directed electric field observed within a WTS. The westward motion of the surge is solely a signature of the expansion of the mangetospheric substorm current system, accelerating plasma earthward progressively towards the flanks of the magnetosphere, which would explain your observations of new forms being actually created west of the old ones, keeping the surge structure up only as a gross pattern. Note also in this context Akasofu's terminology 'westward *travelling* surge' in contrast to 'eastward drifting patches, omega bands, etc.'.

Additional reference

Rostoker, G., Akasofu, S. I., Baumjohann, W., Kamide, Y. & McPherron, R. L. 1988 The roles of direct input of energy from the solar wind and unloading stored magnetotail energy in driving magnetospheric substorms. *Space Sci. Rev.* **46**, 93–111.

PHILOSOPHICAL TRANSACTIONS OF THE ROYAL SOCIETY A MATHEMATICAL, PHYSICAL & ENGINEERING SCIENCES

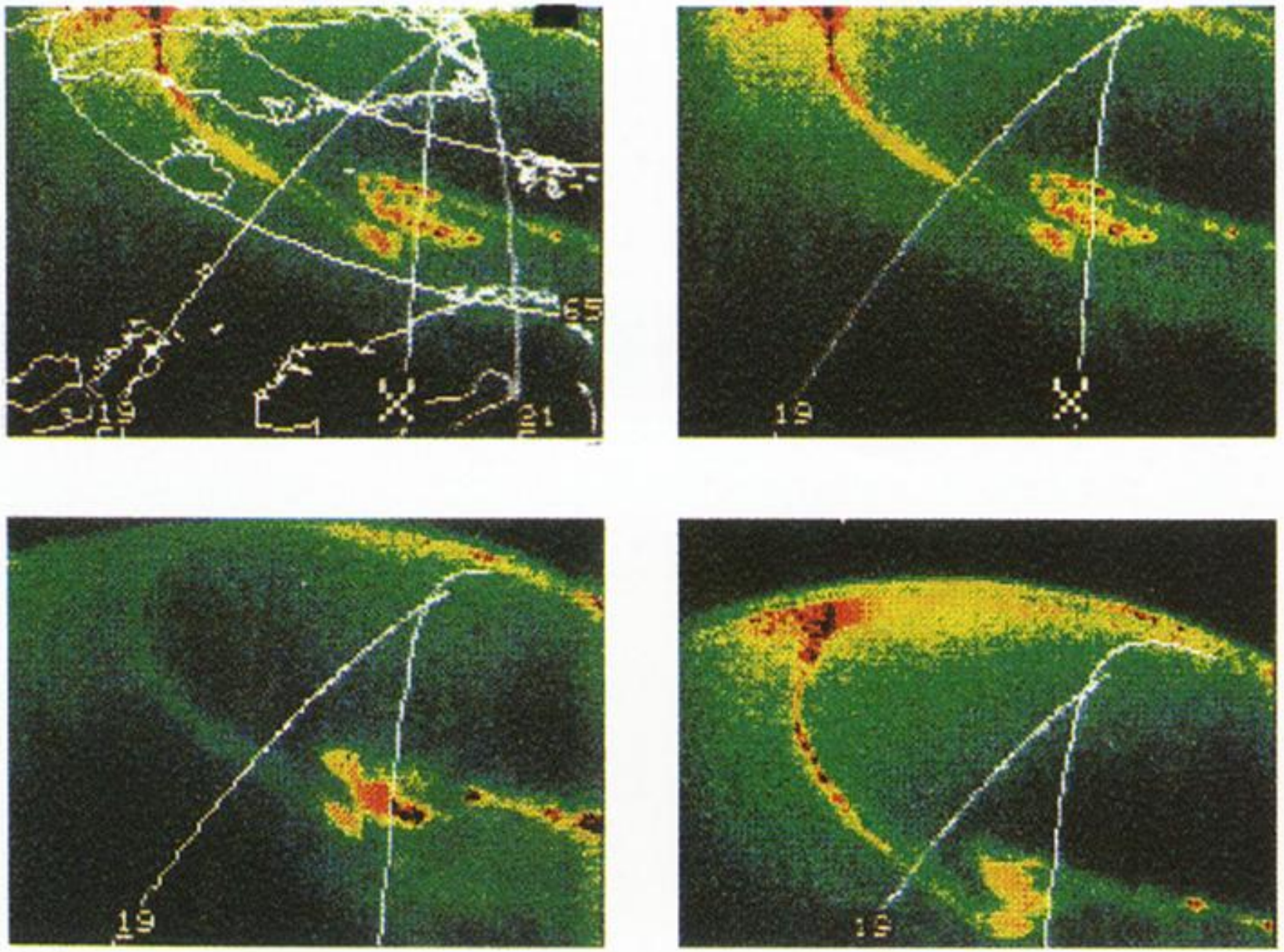

FIGURE 2. Sequence of *Viking* UV-images during orbit 258 on 9 April 1986. In the first two frames the magnetically projected footprint of the *Viking* orbit (position marked with X) is indicated together with the 19h00 and 21h00 magnetic local time (MLT) meridians and map outline. Top left and top right frames are at 18h08:25 U.T.; bottom left is at 18h09:05 U.T.; bottom right is at 18h11:05 U.T.

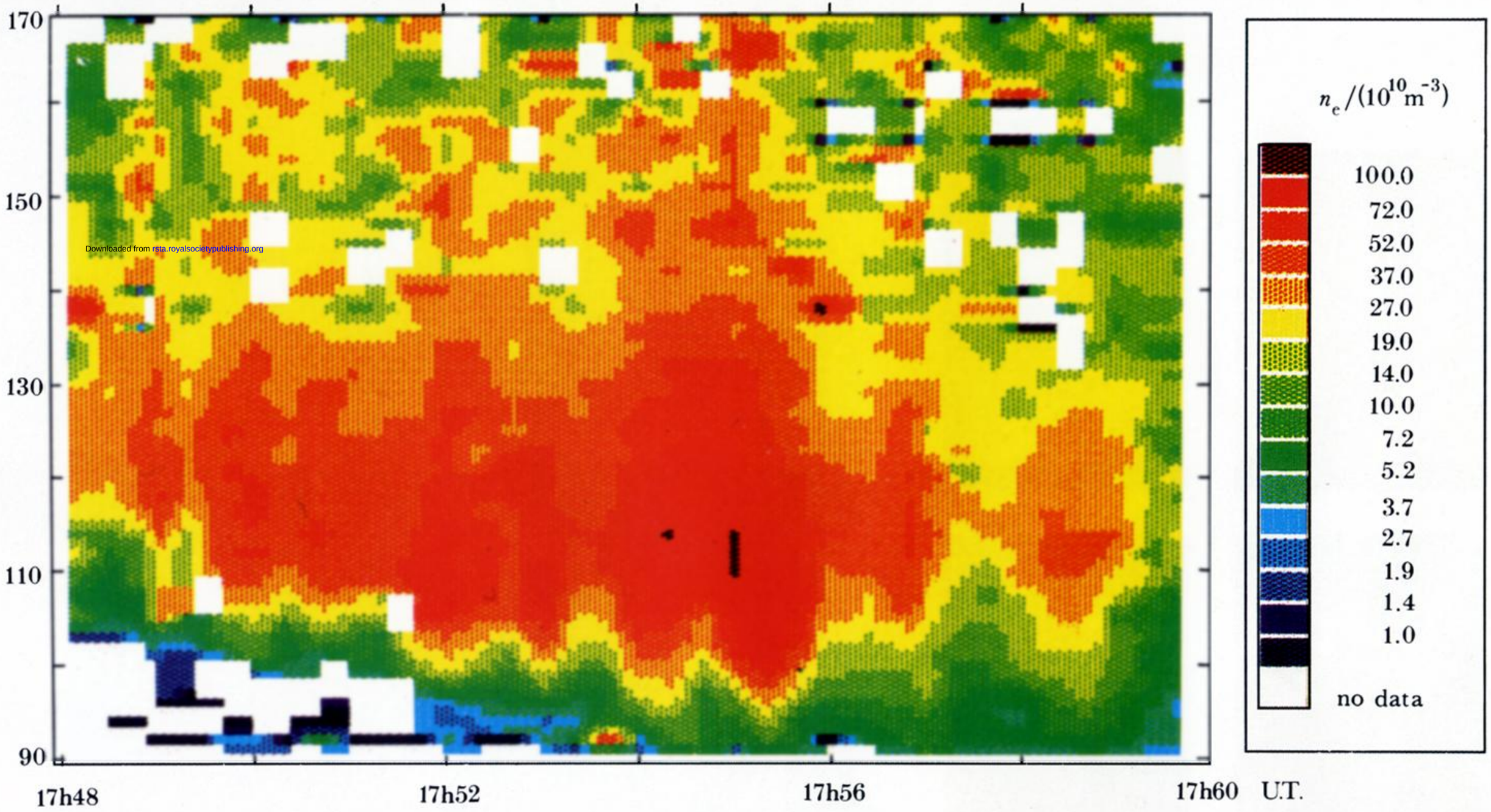

FIGURE 6. Colour-coded plot of ionospheric electron density against altitude and time observed with the E-layer multipulse part of the EISCAT programme UHF1 during the substorm of 9 April 1986.